## CHAPTER 9.

# Causality

"In quantum mechanics... The fundamental equation is itself symmetrical under time reversal... However, despite this symmetry, quantum mechanics does in fact involve an important non-equivalence of the two directions of time. This appears in connection with the interaction of a quantum object with a system which with sufficient accuracy obeys the laws of classical mechanics… If two interactions A and B with a given quantum object occur in succession, then the statement that the probability of any particular result of process B is determined by the result of process A can be valid only if process A occurred earlier than process B." p31 Landau and Lifshitz "Statistical Mechanics".

### 9.1 INTRODUCTION

If *all* the laws of mechanics and quantum mechanics are time reversal symmetric then clearly you cannot prove a time-asymmetric result like the Fluctuation Theorem. In the first proof given by Evans and Searles in 1994 [15], this time symmetry was indeed broken but it was broken in such a natural way that many people who have analysed this proof fail to see where the time reversal symmetry is broken. The assumption made was that processes are *causal* [115].

We quote Landau and Lifshitz above (page 32). This is a statement of the Axiom of *Causality* at least as it applies to quantum mechanics. It is used frequently in quantum mechanics but (unrecognized by Landau and Lifshitz) it is also required in classical mechanics and electrodynamics. The equations of motion in classical (and quantum) mechanics are indifferent to the direction of time – Hamilton's Action Principle shows this with great clarity. However, mechanics on it own does not give us enough information to predict experimental results. We need to know initial or logically, final conditions. When we model laboratory experiments we require initial conditions because this is precisely how the experiments are conducted and because initially, the final state of the system is generally not known. Although we can mimic the effects of time flowing backwards (time decrementing) by applying a time reversal mapping to a set of phases, time nevertheless evolves in a positive sense. Indeed the need to use the time reversal mapping results from the fact that time only increases.

In the proof of the ESFT and the GCFT the probabilities of observing particular values of time integrals of the dissipation function or of the generalised work are computed from the probabilities of observing the initial states from which those sets of trajectories *began*: $f(\mathbf{\Gamma};0)d\mathbf{\Gamma}$. We never used the probabilities of the endpoints; indeed had we done so we would have proved the anti-Fluctuation Theorem and an anti-Second Law [115].

The Axiom of Causality is so natural that people fail to observe that they have made this assumption. Landau and Lifshitz failed to notice that it is constantly used in classical mechanics. This is evidenced by the simple fact that Laplace transforms are only defined by $(0,\infty)$ time integrals rather than $(-\infty,\infty)$ time integrals as used for spatial Fourier transforms. This in turn leads to *memory* functions rather than anti-memory functions. For an extensive discussion of causality and thermodynamics see reference [115].

The Transient Fluctuation Theorem and time dependent response theory are meant to model the following types of experiment. One *begins* an experiment with an ensemble of systems characterised by some *initial* (often equilibrium) distribution function. One *then* does something to the system (applies or turns off a field as the case may be) and one tries to predict what *subsequently* happens to the system. It is completely natural that we assume that the probability of *subsequent* events can be predicted from the probabilities of finding *initial* phases and a knowledge of *preceding* changes in the applied field and environment of the system.

As we will soon see computer simulation provides a clear illustration of the fact that the equations of motion can be run forward or backwards. Those equations of motion are completely time-reversal symmetric. It is the use of causality to predict the outcomes of experiments that breaks the symmetry of time.

**Definition**

The future state of the system is computed solely from the probabilities of states of the system in the past. This is called the *Axiom of Causality*.

It is logically possible to compute the probability of occurrence of present states from the probabilities of future events, but this seems totally unnatural. Will the electric light begin to turn on now, because at some time in the (near) *future*, we *will* throw a switch that applies the necessary voltage? A major problem with this approach is that at any given instant, the future states are generally not known! In spite of these philosophical and practical difficulties, we will explore the logical consequences of the (unphysical) Axiom of *Anticausality*.

We now show that if we derive Green-Kubo relations for the transport coefficients defined by *anticausal* constitutive relations, firstly, these anti-transport coefficients have the opposite sign to their causal counterparts and secondly, the system response starts to change *before* external fields are changed. In an anticausal world it becomes overwhelmingly probable to observe *final* equilibrium microstates that evolved from Second Law violating nonequilibrium steady states. Although this behaviour is *not* seen in the macroscopic world, *anticausal* behaviour is permitted by the solution of the time reversible equations of motion and we demonstrate, using computer simulation, how to find phase space trajectories which exhibit *anticausal* behaviour.

## 9.2 CAUSAL AND ANTICAUSAL CONSTITUTIVE RELATIONS

Consider the component of the linear response at time $t_1$, $dB(t_1)$, of a system characterised by a response function $L(t_1,t_2)$. The response is due to the application of an external force $F$, acting for an infinitesimal time $dt_2(>0)$, at time $t_2$, could be written as,

$$\delta B(t_1) = L(t_1,t_2)F(t_2)\delta t_2. \tag{9.2.1}$$

This is the most general linear, scalar relation between the response and the force components. If the response of the system is independent of the time at which the experiment is undertaken (*i.e.* if the same response is generated when both times appearing in (9.2.1) are translated by an amount t: $t_2 \to t_2 + t, t_1 \to t_1 + t$, then the response function $L(t_1,t_2)$ is solely a function of the difference between the times at which the force is applied and the response is monitored,

$$\delta B(t_1) = L(t_1 - t_2)F(t_2)\delta t_2. \tag{9.2.2}$$

**Definition**

The invariance of the response to time translation is called the *assumption of stationarity*. Equation (9.2.2) does not in fact describe the results of actual experiments because it allows the response at time $t_1$ to be influenced not only by forces in the past, $F(t_2)$, where $t_2 < t_1$ but also by forces that have not yet been applied $t_2 > t_1$ [54]. We therefore distinguish between the causal and anticausal response components,

$$\delta B_C(t_1) \equiv +L_C(t_1 - t_2)F(t_2)\delta t_2, \quad t_1 > t_2 \tag{9.2.3a}$$

$$\delta B_A(t_1) \equiv -L_A(t_1 - t_2)F(t_2)\delta t_2, \quad t_1 < t_2. \tag{9.2.3b}$$

Later, we will prove that $L_C(t) = L_A(-t)$.

Considering the response at time $t$ to be a linear superposition of influences due to the external field at all possible previous (or future) times gives,

$$B_C(t) = \int_{-\infty}^{t} L_C(t - t_1) F(t_1)\, dt_1 \tag{9.2.4a}$$

for the causal response and,

$$B_A(t) = -\int_{t}^{+\infty} L_A(t - t_1) F(t_1)\, dt_1 . \tag{9.2.4b}$$

for the anticausal response.

## 9.3 GREEN-KUBO RELATIONS FOR THE CAUSAL AND ANTICAUSAL RESPONSE FUNCTIONS

And if also the materialistic hypothesis of life were true, living creatures would grow backwards, with conscious knowledge of the future, but no memory of the past

William Thomson, *Nature*, April 9, 1874, pp. 441-444.

To make this discussion more concrete we will discuss Green-Kubo relations for shear viscosity [16]. Analogous results can be derived for each of the Navier-Stokes transport coefficients. We assume that the regression of fluctuations in a system at equilibrium, whose constituent particles obey Newton's equations of motion, are governed by the Navier-Stokes equations.

**Definition**

We consider the *wavevector dependent transverse momentum density*, $J_\perp(k_y,t)$

$$J_\perp(k_y,t) \equiv \sum_i p_{xi}(t) e^{ik_y y_i(t)} \tag{9.3.1}$$

where $p_{xi}$ is the *x*-component of the momentum of particle *i*, $y_i$ is the *y*-coordinate of particle *i* and $k_y$ is the *y*-component of the wavevector. The (Newtonian) equations of motion can be used to calculate the rate of change of the transverse momentum density. They give,

$$\begin{aligned}\dot{J}_\perp &= ik_y[\sum_i p_{xi} p_{yi} e^{ik_y y_i} + \tfrac{1}{2}\sum_{i,j} y_{ij} F_{xij} \frac{1-e^{ik_y y_{ij}}}{ik_y y_{ij}} e^{ik_y y_i}] \\ &\equiv ik_y P_{yx}(k_y,t).\end{aligned} \tag{9.3.2}$$

In this equation $F_{xij}$ is the x-component of the force exerted on particle *i* by particle *j*, $y_{ij} \equiv y_j - y_i$ and $P_{xy}(k_y,t)$ is the *xy*-component of the wavector dependent pressure tensor. For simplicity we assume the interparticle forces are simple pair interactions. For such systems (9.3.2) is exact.

We now consider the response of the pressure tensor to a strain rate, $\dot{\gamma}$, applied to the fluid for $t > 0$ in the causal system and for $t < 0$ in the anticausal system. In the causal system the strain rate is turned on at t = 0 while in the anticausal system the strain rate is turned off at $t = 0$. Since the pressure tensor is related to the time derivative of the transverse momentum current by (9.3.2) and the strain rate is related to the Fourier transform of the transverse momentum density by $\dot{\gamma}(k_y,t) = -ik_y J_\perp(k_y,t)/\rho$, the most general linear, stationary and causal constitutive relation can be written as,

$$\dot{J}_\perp(k_y,t) = \frac{-k_y^2}{\rho}\int_0^t \eta_C(k_y,t-s)J_\perp(k_y,s)ds, \quad t > 0 \tag{9.3.3}$$

where $\eta_C$ is the causal response function (or memory function) and $\rho$ is the mass density. The corresponding anticausal relation is,

$$\dot{J}_\perp(k_y,t) = \frac{k_y^2}{\rho}\int_t^0 \eta_A(k_y,t-s)J_\perp(k_y,s)ds, \quad t < 0 \tag{9.3.4}$$

where $\eta_A$ is the anticausal "response" function. Note that because $t < 0$, we find that the argument ($t$-$s$) in (9.3.4) is less than zero, and we are indeed exploring the response of the system at times less than zero, which is prior to the changes in the strain rate that occur at times greater than zero!

It is straightforward to use standard techniques to evaluate the Green-Kubo relations for the causal and anticausal shear viscosity coefficients.

**Definitions**

In the anticausal case it is important to remember that the usual *Laplace transform*,

$$\tilde{F}(s) \equiv \int_0^{+\infty} F(t)e^{-st}\,dt, \qquad t \geq 0, \tag{9.3.5}$$

is inappropriate and needs to be replaced by an *anti-Laplace transform*,

$$\hat{F}(s) \equiv \int_{-\infty}^{0} F(t)e^{st}\,dt, \qquad\qquad t \le 0. \tag{9.3.6}$$

(Note: $\hat{F}(s) = \int_{0}^{\infty} F(-t)e^{-st}\,dt = \tilde{F}'(s), t \ge 0,$ where $F'(t) \equiv F(-t)$ ). We note that the anti-Laplace transform of a time derivative is $\hat{\dot{F}}(s) = F(0) - s\hat{F}(s)$ and that the anti-Laplace transform of a convolution is the product of the anti-Laplace transforms of the convolutes. By multiplying both sides of equations (9.3.3) and (9.3.4) by $J_{\perp}(-k_y,0)$ and taking an (equilibrium) ensemble average, one can easily derive the following relations for the shear viscosity and the anticausal shear viscosity,

$$\tilde{C}(k_y,s) = \frac{C(k_y,0)}{s + \dfrac{k_y^2 \tilde{\eta}_C(k_y,s)}{\rho}}, \tag{9.3.7a}$$

$$\hat{C}(k_y,s) = \frac{C(k_y,0)}{s + \dfrac{k_y^2 \hat{\eta}_A(k_y,s)}{\rho}} \tag{9.3.7b}$$

where

$$C(k_y,t) \equiv \left\langle J_{\perp}(k_y,t) J_{\perp}(-k_y,0) \right\rangle, \quad \forall t\,. \tag{9.3.8}$$

More useful relations for the viscosity coefficients, especially at $k = 0$, can be obtained by utilising the equilibrium stress autocorrelation function,

$$N(k_y,t) \equiv \frac{1}{Vk_BT} \left\langle P_{yx}(k_y,t) P_{yx}(-k_y,0) \right\rangle, \quad \forall t\,. \tag{9.3.9}$$

Using the fact that $\hat{N} = -\hat{\ddot{C}} / k_y^2 V k_B T$ , one can show [16, 55],

$$\tilde{\eta}_C(k_y,s) = \frac{\tilde{N}(k_y,s)}{1 - k_y^2 \tilde{N}(k_y,s)/\rho s}, \qquad \text{(9.3.10a}$$

$$\hat{\eta}_A(k_y,s) = \frac{\hat{N}(k_y,s)}{1 - k_y^2 \hat{N}(k_y,s)/\rho s}. \tag{9.3.10b}$$

At zero wavevector, we find that the causal and anticausal memory functions are both given by the equilibrium autocorrelation function of the pressure tensor,

$$\begin{aligned} \eta_C(t) &= \eta_A(-t), \quad where\; t > 0 \\ &\equiv \eta(t), \quad \forall t \qquad\qquad (9.3.11) \\ &= \frac{V}{k_B T}\left\langle P_{yx}(t)P_{yx}(0)\right\rangle \end{aligned}$$

where we have used $P_{yx}(t)V = \lim_{k\to 0} P_{yx}(k_y,t)$. Since equilibrium autocorrelation functions are symmetric in time, one does not have to distinguish between the positive and negative time domains. This proves our assertion made in §9.2 that $L_C(t) = L_A(-t)$.

Using equations (6.3.2)–(6.3.4) and taking the zero wavevector limit, we obtain the causal response of the *xy*-component of the pressure tensor,

$$P_{yxC}(t) = -\int_0^t \eta(t-s)\dot{\gamma}(s)ds \qquad t > 0 \qquad (9.3.12)$$

and the anticausal response is,

$$P_{yxA}(t) = \int_t^0 \eta(t-s)\dot{\gamma}(s)ds \qquad t < 0\,. \qquad (9.3.13)$$

In the linear regime close to equilibrium the instantaneous dissipation function, $\Omega(t)$, is given by,

$$\Omega(t) = -\beta P_{yx}(t)\dot{\gamma}(t)V\,, \qquad (9.3.14)$$

where $\dot{\gamma}(t)$ is the time dependent strain rate. From equations (9.3.12) and (9.3.13), it is easy to see that if we conduct two shearing experiments, one on a causal system with a strain rate history $\dot{\gamma}_C(t)$ and one on an anticausal system with $\dot{\gamma}_A(t) = \pm\dot{\gamma}_C(-t)$, then

$$\Omega_A(t) = -\Omega_C(-t)\,. \tag{9.3.15}$$

This proves that if the causal system satisfies the Second Law of Thermodynamics then the anticausal system must violate that Law and vice versa. If we now invoke the Second Law Inequality we see the following:

$$\int_0^t ds\,\langle \Omega_A(-s)\rangle = -\int_0^t ds\langle \Omega_C(s)\rangle \le 0, \quad \forall t > 0\ . \tag{9.3.16}$$

**Definition**

Equation (9.3.16) is the *AntiSecond Law Inequality*.

## 9.4 EXAMPLE: THE MAXWELL MODEL OF VISCOSITY

In this section we examine the consequences of the causal and anticausal response by considering the Maxwell model for linear viscoelastic behaviour [16]. If we consider the causal response of a system to a two step strain rate ramp:

$$\begin{aligned} &\dot{\gamma}_C(t) = a \qquad 0 < t < t_1 \\ &\dot{\gamma}_C(t) = b \qquad t_1 < t < t_2 \end{aligned} \tag{9.4.1}$$

then use the Maxwell memory kernel,

$$\eta_M(t) = G_\infty e^{-|t|/\tau_M}, \quad \forall t \tag{9.4.2}$$

in (9.3.12) and the fact that the causal, $\eta_C$, and anticausal, $\eta_A$, Maxwell shear viscosities in the zero frequency limit are

$$\eta_C = \eta_A = G_\infty \tau_M = \eta_M, \tag{9.4.3}$$

we find that the causal response is:

$$P_{xyC}(t) = -a\eta(1 - e^{-t/\tau_M}), \quad 0 < t < t_1$$

$$P_{xyC}(t) = -a\eta(e^{-(t-t_1)/\tau_M} - e^{-t/\tau_M}) - b\eta(1 - e^{-(t-t_2)/\tau_M}), \quad t_1 < t < t_2. \tag{9.4.4}$$

If we now consider the corresponding anticausal experiment with strain rate histories given by:

$$\begin{aligned} &\dot{\gamma}_A(t) = a \qquad -t_1 < t < 0 \\ &\dot{\gamma}_A(t) = b \qquad -t_2 < t < -t_1 \end{aligned}. \tag{9.4.5}$$

We find that the anticausal response is:

$$P_{xyA}(t) = a\eta(1 - e^{t/\tau_M}), \quad -t_1 < t < 0$$

$$P_{xyA}(t) = a\eta(e^{(t+t_1)/\tau_M} - e^{t/\tau_M}) + b\eta(1 - e^{(t+t_2)/\tau_M}), \quad -t_1 < t < -t_2 . \qquad (9.4.6)$$

From equations (9.4.4) and (9.4.6) it is clear that,

$$P_{xyA}(t) = -P_{xyC}(-t) . \qquad (9.4.7)$$

These response functions are shown graphically in figure 9.4.1. A two step strain rate ramp with $a$ = 1.0, $b$ = 0.5, $t_1$ = 2 and $t_2$ = 4 was considered. Equations (9.4.4) and (9.4.6) were used to predict the causal and anticausal responses, respectively, of the *xy*-component of the pressure tensor. Values of $G_\infty$ = 40.0 and $t$ = 0.05 were used in the model. These values were obtained from approximate fits to computer simulation data (see §6.5).

The data in figure 9.4.1 show that for the causal response, $P_{xy}$ is zero at equilibrium ($t \le 0$) and decreases when the field is applied until the steady state value is obtained. It remains at the steady value until $t$ = 2, at which time the strain rate is reduced. Since this system is causal, no change in $P_{xy}$ occurs until *after* the strain rate is reduced, when it increases until the system reaches a new steady state. We display the anticausal response from $t$ = -4 where it is in an antisteady state. Just *before* the strain rate is increased (at $t$ = -2), $P_{xy}$ increases to a new antisteady state value. Using equation (9.3.14) we see that in the causal response dissipation is in the graph always positive and Second Law satisfying, whereas in the anticausal response the instantaneous dissipation is in this graph always negative.

a. Causal

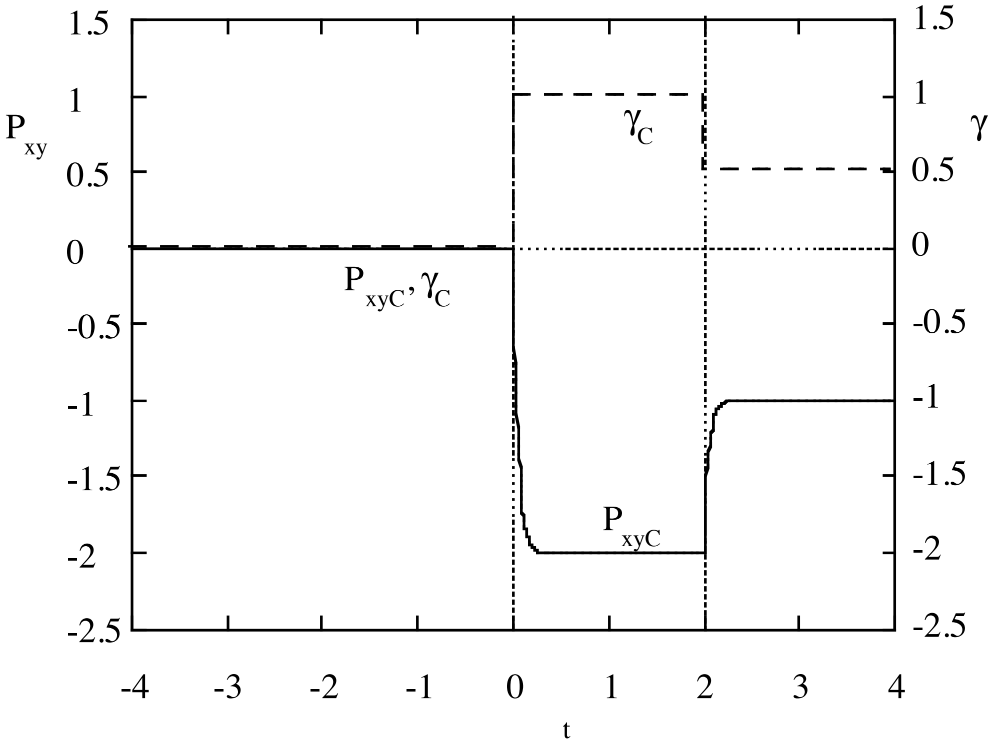


b. Anticausal

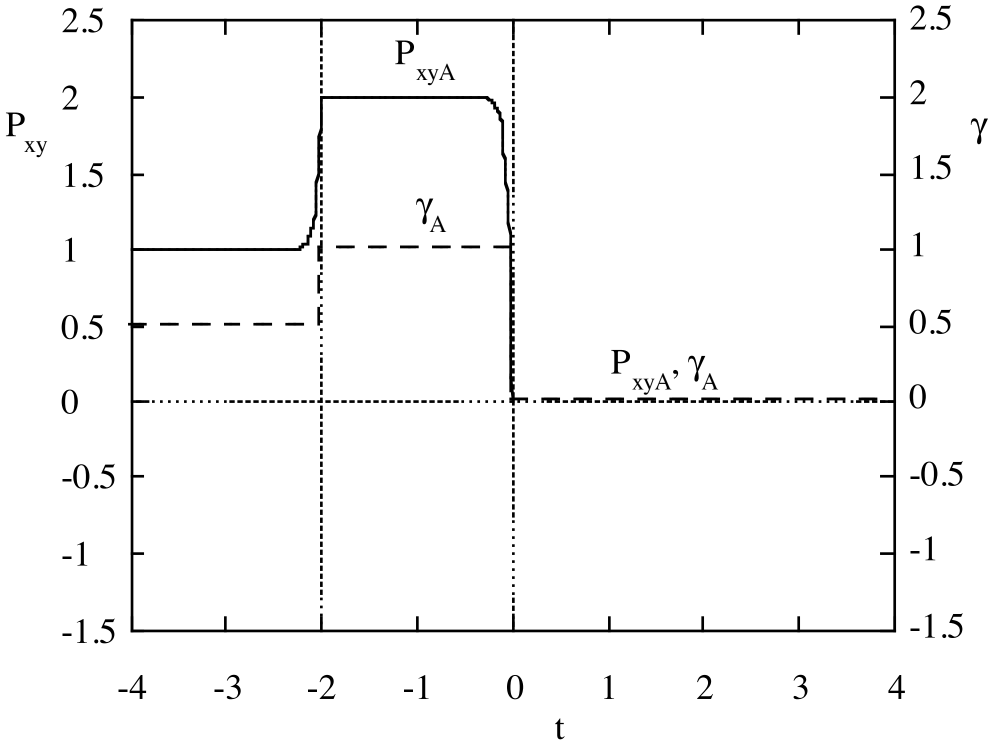

**Figure 9.4.1** A schematic diagram of the (a) causal and (b) anticausal response of $P_{xy}$ to a two step strain rate ramp determined using the Maxwell model for linear viscoelastic behaviour with $G_\infty$ = 40 and $\tau_M$ = 0.05 (solid line). In both cases the time dependence of the strain rate is shown as a dashed line.

## 9.5 PHASE SPACE TRAJECTORIES FOR ERGOSTATTED SHEAR FLOW

We now examine the causal and anticausal response on a microscopic scale and we consider the relative probability of observing Second Law satisfying and Second Law violating trajectories by studying a ergostatted system of N particles under shear.

The ergostatted SLLOD equations of motion (2.3.1), (2.3.3) are time reversible [16]. Therefore for every *i*-segment $S^t\boldsymbol{\Gamma}_{(i)}$, $(0 < t < \tau)$, there exists a conjugate trajectory segment $S^t\boldsymbol{\Gamma}_{(i^{(K)})}, (0 < t < \tau)$ with the property that, $P_{xy}(S^t\boldsymbol{\Gamma}_{(i^{(K)})}) = -P_{xy}(S^{-t}\boldsymbol{\Gamma}_{(i)}), (0 < t < \tau)$. Thus, the t-averaged shear stress $\bar{P}_{xy,i,t} \equiv \frac{1}{t}\int_0^t ds\, P_{xy}(S^s\boldsymbol{\Gamma}_i)$ for segment i is equal and opposite to that for its conjugate: $\bar{P}_{xy,i^K,t} = -\bar{P}_{xy,i,t}$. We note that since the solution of the equations of motion is a unique function of the initial conditions the conjugate segment is also unique.

We have previously shown that for shear flow conjugate segments may be generated by using a phase space mapping known as a Kawasaki- or K-map [16]. A K-map of a phase, $\boldsymbol{\Gamma}$, is defined as a time-reversal map which is followed by a y-reflection. In the case of shear flow the K-map leaves the strain rate unchanged but changes the sign of the shear stress, that is $M^K\boldsymbol{\Gamma} = M^K(x,y,z,p_x,p_y,p_z) = (x,-y,z,-p_x,p_y,-p_z) \equiv \boldsymbol{\Gamma}^{(K)}$ [16]. It is straightforward to show that the Liouville operator for the system simulated by equations (2.3.1) and (2.3.3), $iL(\boldsymbol{\Gamma},\dot{\gamma}) \equiv \sum\left[\dot{\mathbf{q}}_i(\boldsymbol{\Gamma},\gamma)\bullet\partial/\partial\mathbf{q}_i + \dot{\mathbf{p}}_i(\boldsymbol{\Gamma},\dot{\gamma})\bullet\partial/\partial\mathbf{p}_i\right]$, has the property that under a *K*-map, $M^{(K)}iL(\boldsymbol{\Gamma},\dot{\gamma}) = iL(\boldsymbol{\Gamma}^{(K)},\dot{\gamma}^{(K)}) = -iL(\boldsymbol{\Gamma},\dot{\gamma})M^{(K)}$. If we assume a strain rate history such that, $\dot{\gamma}_K(-t) = \dot{\gamma}(t) \quad \forall t$, then it follows that if a *K*-map is carried out on an arbitrary phase, $\mathbf{\Gamma}$ at $t = 0$ then evolution *forward* in time from $\mathbf{\Gamma}^{(K)}$ under a strain rate $\dot{\gamma}_K(t)$ is equivalent to time evolution *backwards* in time from $\mathbf{\Gamma}$ under the strain rate history $\dot{\gamma}(t)$, ($t$<0),

$$P_{xy}(-t,\mathbf{\Gamma},\dot{\gamma}(-t)) = \exp[-iL(\mathbf{\Gamma},\dot{\gamma}(-t))t]P_{xy}(\mathbf{\Gamma}) = -P_{xy}(t,\mathbf{\Gamma}^{(K)},\dot{\gamma}_K(t)) \qquad (9.5.1)$$

We note that if we do not assume that $\dot{\gamma}_K(-t) = \dot{\gamma}(t)\ \forall t$, then there is no general method for generating conjugate trajectory segments. This is because propagators with different strain rates do not commute and the inverse propagator must therefore retrace the strain rate history of the conjugate propagator but in inverse historical order.

We will now indicate in more detail, how to construct the conjugate segment, $i^{(K)}$, from an arbitrary phase space trajectory segment $i$ [32]. The construction is illustrated in figure 9.5.1 for the case where the strain rate remains the same for the duration of the trajectory. A trajectory of length τ is generated by solving the equations of motion. The conjugate segment is then constructed by applying a K-map to the phase at the midpoint of the segment ($t = \tau/2$), $M^K\mathbf{\Gamma}_{(2)} = \mathbf{\Gamma}_{(5)}$. We then advance in time from the point ($\mathbf{\Gamma}_{(5)}$), to $t = \tau$, by solving the equations of motion and also go backwards in time from the K-mapped point, $t = \tau/2$, to $t = 0$. A conjugate trajectory of length $\tau$ is thereby produced. This construction has previously been described in more detail [32].

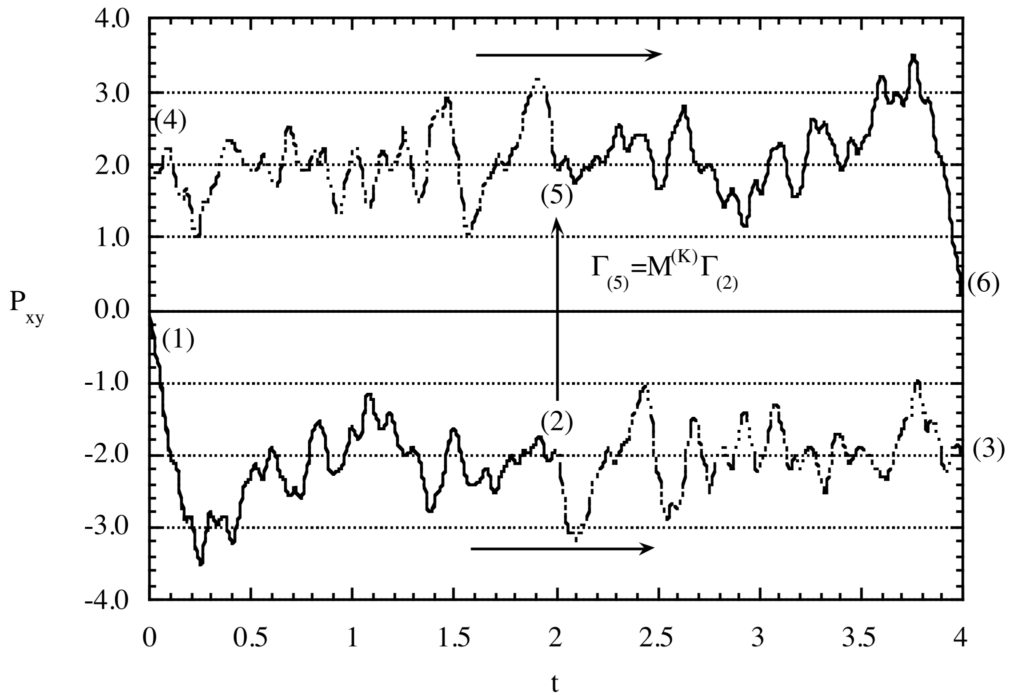


**Figure 9.5.1** $P_{xy}$ for trajectory segments from a simulation of 200 disks at $T$ = 1.0 and $n$ = 0.8. A constant strain rate of $\gamma$= 1.0 is applied at $t$ = 0. The trajectory segment $\mathbf{\Gamma}_{(1,3)}$ was obtained from a forward time simulation. At $t$ = 2, a $K$-map was applied to $\mathbf{\Gamma}_{(2)}$ to give $\mathbf{\Gamma}_{(5)}$. Forward and reverse time simulations from this point give the trajectory segments $\mathbf{\Gamma}_{(5,6)}$ and $\mathbf{\Gamma}_{(5,4)}$, respectively. If one inverts $P_{xy}$ in $P_{xy}$ = 0 and inverts time about $t$ = 2, one transforms the $P_{xy}(t)$ values for the antisegments $\mathbf{\Gamma}_{(4,6)}$ into those for the conjugate segment $\mathbf{\Gamma}_{(1,3)}$.

Clearly, the mapped trajectory is a solution of the equations of motion for the system, and therefore it would eventually be observed from the ensemble of starting states. When the $K$-map is carried out at $t$ = 0, the shear stress is inverted and equation (6.5.1) shows that $P_{xy}(\tau/2+t,\mathbf{\Gamma})=-P_{xy}(\tau/2-t,\mathbf{\Gamma}^{(K)})$ and similarly $P_{xy}(\tau/2-t,\mathbf{\Gamma})=-P_{xy}(\tau/2+t,\mathbf{\Gamma}^{(K)})$, therefore for every point on the original trajectory there is a unique point on the mapped trajectory with opposite shear stress. The $\tau$-averaged shear stress of the conjugate trajectory is opposite to that of the original trajectory, that is $\overline{P}_{xy,i^K}(\tau) = -\overline{P}_{xy,i}(\tau)$. Thus, if the original segment was a Second Law satisfying segment then the conjugate segment is a Second Law violating segment, and vice versa.

In a *causal* world, which is described by causal macroscopic constitutive relations such as (9.2.4), observed segments are overwhelmingly likely to be Second Law satisfying. It is a simple matter to apply the arguments of §2.1 for the special case of ergostatted shear flow where a simple time reversal map cannot be used, and must be replaced by the K-map (see footnote 8). The condition of ergodic consistency has to be modified slightly to require:

$$f(S^t \boldsymbol{\Gamma}^K;0) \neq 0, \forall \boldsymbol{\Gamma} \in D \,. \qquad (9.5.2)$$

The result is the TFT given in (2.1.11).

## 9.6 SIMULATION RESULTS

We can demonstrate the relationships between the conjugate pairs of trajectories, the Second Law of Thermodynamics and causal and anticausal response using numerical simulations of the system described by equations (1.3.1) and (1.3.2). Figure 6.5.1 shows the response of $P_{xy}$ for a trajectory and its conjugate when a constant strain rate is applied. The response was determined using nonequilibrium molecular dynamics simulations of 200 disks in two Cartesian dimensions. The disks interact via the WCA potential [45],

$$\phi(r) = \begin{cases} 4(r^{-12} - r^{-6}) + 1 & r < 2^{1/6} \\ 0 & r > 2^{1/6} \end{cases} \tag{9.6.1}$$

Shearing periodic boundary conditions were used to minimise boundary effects [16]. The system was maintained at a constant kinetic temperature of $T = 1.0$ and the particle density was $n = N/V = 0.8$. An initial phase was selected from an equilibrium distribution and a strain rate of $\gamma = 1.0$ was applied to the system at $t = 0$. A trajectory segment was generated by simulating forward in time to $t = 4$. The conjugate trajectory was constructed using the scheme describe above. Examination of the trajectories shows that $P_{xy}(\tau + t)$ for the Second Law satisfying trajectory is equal in magnitude but opposite in sign to $P_{xy}(\tau - t)$ for the Second Law violating trajectory, where $t$ is the time at which the $K$-map is applied ($\tau = 2$). These results therefore confirm the relationship between $P_{xy}$ of Second Law satisfying trajectories and Second Law violating conjugate trajectories given by equation (6.5.1).

The causality of the response is more clearly demonstrated in figure 6.6.1 where the response of $P_{xy}$ to a strain rate ramp is shown. $P_{xy}(t)$ was averaged over a 100 individual trajectories to reduce the fluctuations in the steady state and giving a partially ensemble averaged response $\overparen{P_{xy}(t)}$. In these simulations 56 disks were used. The initial phases of the trajectories shown in figure 6.6.1 were sampled from the equilibrium distribution at t = 0. $\overparen{P_{xy}}$ is close to zero at equilibrium and decreases to near a steady state value after the field is applied. After the strain rate is reduced, $\overparen{P_{xy}}$ increases towards a new steady state value.

The conjugate trajectories are shown in figure 9.6.1. They were constructed as described above and translated in time to begin at *t* = -4. At this time, the system is in an antisteady state and $\overparen{P_{xy}}$ remains near its antisteady state value until just <u>*before*</u> the the strain rate is changed, when it increases towards a new antisteady state value.

In accord with the TFT, these response curves demonstrate that most initial phases (here all 100 randomly selected initial phases) satisfy the Second Law and most phases (again all 100 initial random phases) exhibit response curves that we would describe as having "causal" characteristics (*i.e.* the stress responds to *prior* rather than *future*, changes in the strain rate). Second Law violating conjugate trajectories respond to the step in the strain rate <u>*before*</u> it is made, so they are <u>*anticausal*</u>. Close inspection of the graph reveals that at all points along pairs of conjugate trajectories, $P_{xy}(t)_{trajectory} = -P_{xy}(-t)_{conjugate\ trajectory}$ which follows from (9.5.1).

a. Causal

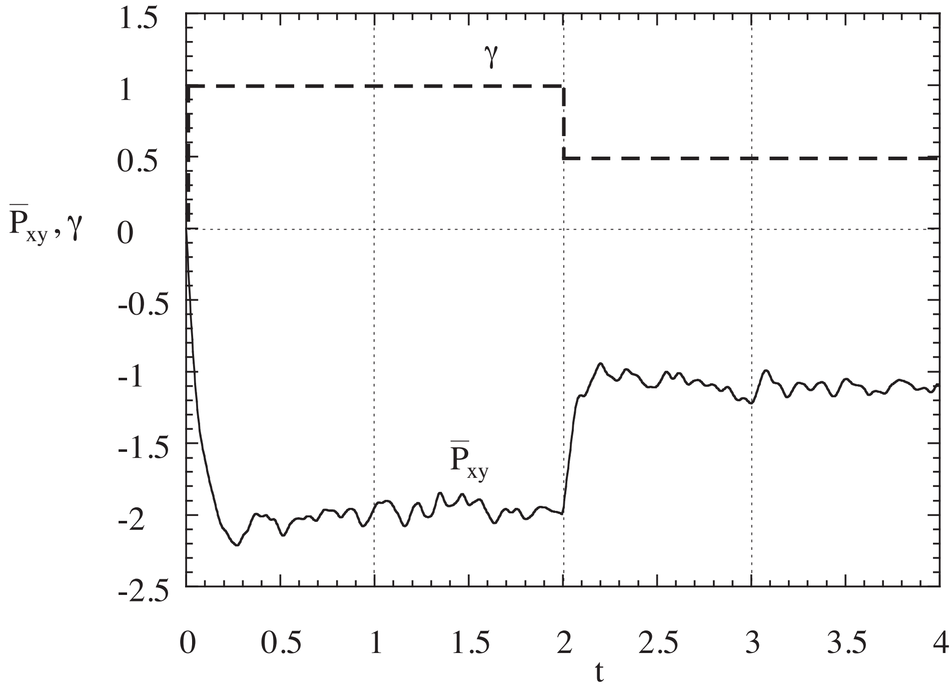

1.5
1
0.5
0
-0.5
-1
-1.5
-2
-2.5
$\overline{P}_{xy}, \gamma$
$\gamma$
$\overline{P}_{xy}$
0
0.5
1
1.5
2
2.5
3
3.5
4
t

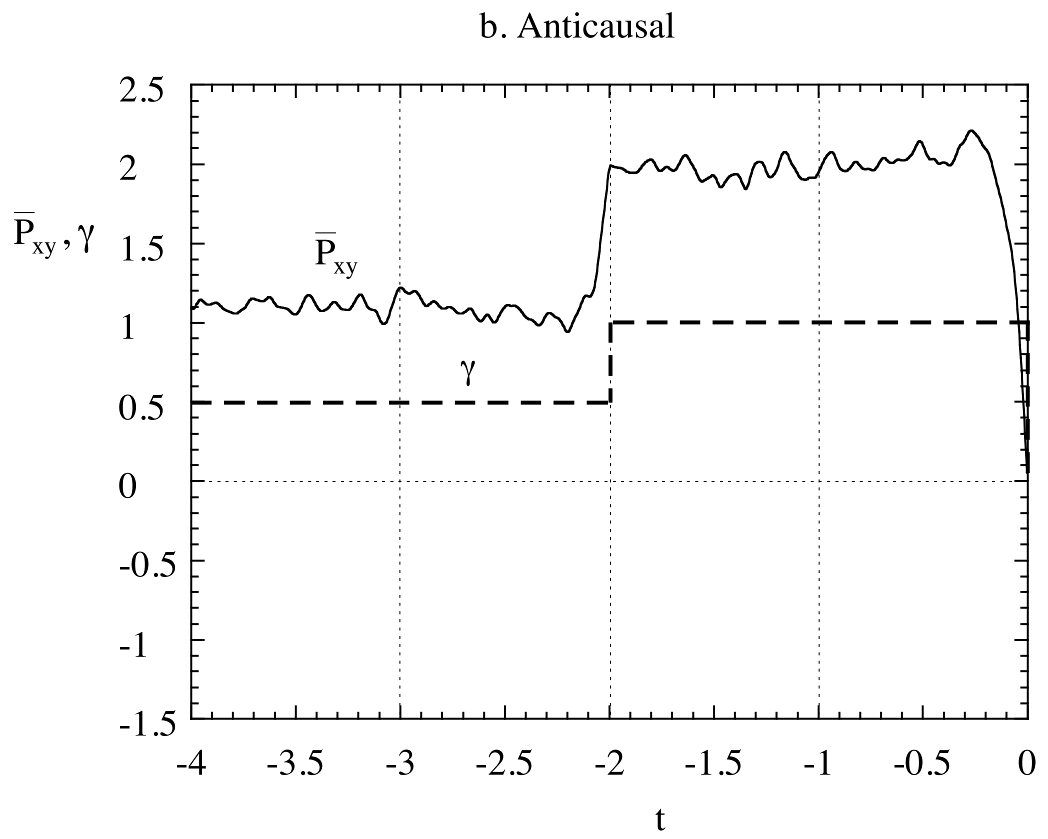


**Figure 9.6.1** $\overline{P}_{xy}$ (solid line) from nonequilibrium molecular dynamics simulations of 56 particles at $T = 1.0$ and $n = 0.8$ undergoing shear flow. The dashed line gives the time-dependence of the strain rate. In (a) $\overline{P}_{xy}$ was determined using 1000 trajectories whose initial phases were selected from an equilibrium distribution, and to which a two step strain rate was applied. (b) shows $\overline{P}_{xy}$ for their conjugate trajectories. The conjugate trajectories were obtained by applying a $K$ map to the phase of the trajectory at $t = 2$, simulating forward and backward in time from this point and translating in time so that the conjugate trajectory ends at $t = 0$. Note that the strain rate history of the conjugate trajectory is reversed.

The system used in the simulations corresponds to that examined using the Maxwell model described in §9.4. Figure 9.6.1 shows the response, determined by nonequilibrium molecular dynamics simulation, to the same two step strain rate ramp which was used to model the response shown in figure 9.4.1. Comparison of these response curves indicates that the system is reasonably well represented by the Maxwell model.

We should also note that if we generate an antitrajectory, that has negative average dissipation, such a trajectory will not continue indefinitely. Because the sum of it's Lyapunov exponents is positive while the sum of exponents for the trajectory is negative, the antitrajectory is less mechanically stable than its conjugate trajectory. Because no numerically computed trajectory is exact, this numerical error is amplified by the Lyapunov instability and eventually the antitrajectory will decay into a trajectory with positive average dissipation.

If the error in any computed phase space position is $\delta$ and if the particles have a dimensionless radius and average momentum of unity, the time required for the antitrajectory to decay is $\delta / \lambda_{\min}$ where $\lambda_{\min}$ is the smallest (*i.e.* the most negative) Lyapunov exponent for the trajectory with positive average dissipation. This decay has nothing to do with why the Second "Law" is satisfied. The error $\delta$ is not a material property. In an electrical circuit the Second "Law" is satisfied immediately the voltage $F_e$, is applied. In fact the initial rate of increase in the electrical current desnsity $J$, is given by an equilibrium fluctuation formula which has nothing to do with noise of errors, or Lyapunov instability: $\lim_{t \to 0^+} d\left\langle J(t) \right\rangle / dt = -\beta V \left\langle J(0^-)^2 \right\rangle_{eq} F_e$.

One might have thought that the instability of the antitrajectory would be very strong and the slope $d\left\langle J \right\rangle / dt$, when the current crosses zero, would be very large. In fact this is not so and the crossing slope is typically much less than the initial slope caused by applying the voltage to the system which was at equilibrium at time zero!

## 9.7 SUMMARY AND CONCLUSION

As we have seen throughout this book, it is dissipation and not phase space compression, entropy or entropy production that features in the Fluctuation, Dissipation and Relaxation Theorems. Each of these theorems is exact for systems of arbitrary size and arbitrarily near or far from equilibrium. It used to be said that for nonequilibrium systems virtually no exact results are known. This is most definitely not the case today.

At the end of this book we are now in a position to identify the key quantity that facilitates the entire exposition. Dissipation dominates the theory. Although it was originally defined to give the probability ratios of observing in the same initial ensemble, sets of trajectories and their conjugate anti-trajectories, this definition (3.1.2) also involves a balance between energy change and phase space volume (6.3.4). This is particularly obvious in equilibrating systems (5.4.10). By loosing a certain quantity of heat from an otherwise Hamiltonian system, the system also gives up a certain amount of phase space. The ratio of heat loss to phase space expansion is given by $k_B T$ the reciprocal of the integration factor for the heat appearing in the Clausius Inequality.

This quantity $k_B T$ is also involves the equilibrium thermodynamic temperature the nonequilibrium system will relax towards if any dissipative field is set to zero immediately, and the entire system is allowed to relax towards equilibrium. This underlying equilibrium temperature is another key element of our theory.

The Fluctuation Theorems are proved by directly exploiting the time reversal symmetry of the dynamics. Time reversed sets of trajectories and antitrajectories are actually exploited to prove the theorem. Indeed is systems where these conjugate sets do not exist, the fluctuation relations are not valid – ergodic consistency has broken down. Indeed the theorems are so powerful and general, precisely because their proofs make so few assumptions.

The other feature of our thesis is the minor role played by entropy. Indeed entropy was only mentioned for systems at equilibrium (§5.2,4). Indeed since Gibbs' Second Paradox was announced (that entropy is preserved by Hamiltonian dynamics), entropy has been problematic away from equilibrium. Our thesis is that it is unnecessary to consider entropy, except for equilibrium systems where dissipation on the other hand, is identically zero. Entropy and dissipation are thus seen to have perfectly complementary roles.

It seems astonishing that 176 years after Clausius made his famous remarks: "*The energy of the Universe is constant. The entropy of the Universe tends to a maximum.*" that we have now come to such a different point of view. The ubiquity of Clausius' view is also even more astonishing because of the criticisms of his arguments that were already made in the late 19th century.

*The energy and the entropy are both constants of the motion but on average, the time integrated dissipation increases until at sufficiently late times in any isolated system it is constant.* We have also at last come to realize the fundamental role played by Causality in physics. The so-called laws of physics are by themselves insufficient to predict what goes on in the Universe. Those laws must be supplemented with the Axiom of Causality in order to predict the outcomes of experiments. This Axiom is so natural that physicists almost always fail to realize that it is in fact an assumption and that an alternative possibility is logically possible.

This lack of recognition is however, precisely why the proof of the "laws" of thermodynamics had to wait so long.